Energy Reports 8 (2022) 13529–13543

Contents lists available at ScienceDirect

Energy Reports

journal homepage: www.elsevier.com/locate/egyr

Research paper

Highly efficient maximum power point tracking control technique for PV system under dynamic operating conditions

Syed Kumayl Raza Moosavi [a,1], Majad Mansoor [b,1], Muhammad Hamza Zafar [c,1], Noman Mujeeb Khan [c,1], Adeel Feroz Mirza [d,1], Naureen Akhtar [e,*,1]

[a] Department of Mechatronics, National University of Sciences and Technology, Islamabad 44000, Pakistan
[b] Department of Automation, University of Science and Technology of China, Hefei 230027, China
[c] Department of Electrical, Capital University of Science and Technology, Islamabad 44000, Pakistan
[d] Department of Power Electronics and Electrical Machines, Gdansk University of Technology, Poland
[e] Department of Engineering Sciences, University of Agder, Grimstad, Norway

ARTICLE INFO

Article history:
Received 23 March 2022
Received in revised form 4 July 2022
Accepted 2 October 2022
Available online xxxx

Keywords:
Partial shading (PS)
Particle swarm optimization (PSO)
Maximum power point tracking (MPPT)
Swarm intelligence (SI)
Dynamic group-based cooperative optimization (DGBCO)
Relative error (RE)

ABSTRACT

The application of small-scale electrical systems is widespread and the integration of Maximum Power Point Tracking (MPPT) control for Photovoltaic systems with battery applications further enhances the techno-economic feasibility of renewable systems. For this purpose, a novel MPPT control system using Dynamic Group based cooperation optimization (DGBCO) algorithm is utilized for PV systems. The population in the DGBCO is divided into exploration and exploitation groups. Due to effective mathematical modeling, the drawbacks of existing MPPT control techniques are undertaken. The drawbacks of modern MPPT control become prominent under partial shading conditions (PSC) which give rise to power loss, random fluctuations, and slow control action. The DGBCO is implemented using a search and skip mechanism which significantly enhances the performance of the MPPT controller and improves the efficiency of PV systems. The results are compared with recently developed Artificial Bee Colony (ABC), Cuckoo Search Algorithm (CS), DragonFly Optimizer (DFO), and Particle Swarm Optimization (PSO) techniques. The operating conditions case studies include fast varying irradiance and PS with skewed GM. The DGBCO based MPPT control technique is also validated by the experimental setup. The results are compared using statistical and analytical indices such as tracking time, settling time, power tracking efficiency, total energy, RMSE, MAE, and RE. The results show the superior performance of the proposed DGBCO. Relatively, 2%–8% higher energy harvest, and up to 60% faster tracking time helps to achieve up to 99.86% power tracking efficiency in both transient and steady-state control operation. Lower values of statistical metrices i.e. RMSE, MAE, and SR indicate the robustness and effective mathematic modeling of DGBCO for effective MPPT of PV systems under PS conditions.

1. Introduction

Resources of the Earth are gradually but surely depleting. In growing societies, much focus has been shifted on the research and development of energy consumption. Non-renewable resources are no longer considered a viable source for fuel and hence for the purposes of flourishment of future generations, renewable energy has become the main ingredient (Agyekum, 2021). Amongst all the types of non-renewable energy resources such as Nuclear, Wind, Biofuels, and Solar. Solar energy has been the target of much research and debate. This is primarily due to the fact that the Solar Photovoltaic (SPV) energy source is fuel-free, requires minor maintenance, is free of rotary or moving parts, and causes no pollution to the environment (Vicente et al., 2020; Mendez et al., 2020; Yang et al., 2020).

From an application standpoint, the SPV energy system can be categorized into four distinct types: Stand-alone low power plants, remote small SPV plants, large-scale grid-connected plants (Matayoshi et al., 2020), and a hybrid of SPV and other renewable/non-renewable energy sources (Belhachat and Larbes, 2018; Rezk et al., 2017). In any case, for any smart home system, a constant flow of power is required. This can only be met by the arrangement of a system of batteries to supply stored energy to

* Corresponding author.
E-mail addresses: moosavi7@hotmail.com (S.K.R. Moosavi), majad@mail.ustc.edu.cn (M. Mansoor), hamzauetms@gmail.com (M.H. Zafar), naumanmujeebk@gmail.com (N.M. Khan), adeel.mirza@pg.edu.pl (A.F. Mirza), naureen.akhtar@uia.no (N. Akhtar).

[1] All authors were involved in the preparation and review of the original manuscript.

https://doi.org/10.1016/j.egyr.2022.10.011

Abbreviations and Variables

Abbreviations

DFO	Dragonfly optimization
CSA	Cuckoo search optimization algorithm
FOCV	Fractional open circuit voltage
FSCC	Fractional short circuit current
GM	Global maxima
GMMP	Global maximum power point
GWO	Grey wolf optimizer
IPSO	Improved particle swarm optimization
LM	Local maxima
LMPP	Local maxima power point
MAE	Mean absolute error
MPPT	Maximum power point tracking
P&O	Perturb and observe
PS	Partial shading
RE	Relative error
RMSE	Root mean square error
SR	Success Rate
DGBCO	Dynamic group based optimization algorithm

Variables

a	Diode ideality factor
G_{STC}	Irradiance at STC condition ($1000\ W/m^2$)
G	Irradiance (W/m^2)
I_{PV}	Cell current
I_{PV-STC}	Cell current at STC conditions
I_d	Diode current
I_o	Reverse saturation current
I_{out}	Output current
K_I	Short circuit current constant
k	Boltzmann constant $= 1.38073 \times 10^{-23}$ J/K
N_p	Number of cells in parallel connection
N_s	Number of cell connected in series
q	Electron charge $= 1.6022 \times 10^{-19}$ C
R_p	Equivalent parallel resistance cell
R_{peq}	Total Equivalent parallel resistance array
R_s	Equivalent series resistance cell
R_{seq}	Equivalent series resistance array
T_{STC}	Temperature at STC condition (25 °C)
T	Temperature (°C)
V_T	Thermal voltage of the PV module
V_{out}	Output voltage

homes during poor weather conditions or during peak loading states. On the other hand, during peak irradiance conditions and/or low loading state, batteries store the extra power.

The process of storing and delivering energy from the SPV array to batteries is paramount to the overall efficiency of the system (Atri et al., 2020). The point where the SPV array operates at its maximum power output point is called Maximum Power Point (MPP) (Golla et al., 2021). Different soft computing techniques have been applied in recent years to guarantee maximum Power output for battery charging in different renewable energy sources such as Fuel cells, Thermoelectric (TEG), and PV systems. Classical Constant Current and Voltage Charging based MPPT methods in which SPV are directly connected with the battery and load which trail in efficiency (Premkumar et al., 2020).

However, most studies do not consider the underlying fact that solar irradiation in practical terms is not fixed (Fathabadi, 2020). For example, Kumar et al. (2021b) suggests that MPP current is tracked when the battery is being charged and once the charging limit is met, the control switches to a constant voltage supplying mode. Another method proposes work on the maximum power theorem i.e. maximum power to be transferred when the load resistance is equal to internal resistance. Such methods of MPP tracking (MPPT) for battery charging cannot be employed at variable solar irradiance and temperature conditions (Kim et al., 2021).

1.1. Literature review

Due to the deficiency of a constant high irradiation source, research has been carried out for the MPPT of partial shading conditions through the use of DC–DC converters (Kumar et al., 2021a). The power of the SPV panels is fed into the battery via a DC–DC converter as presented in Fig. 1. The operating point of the converter for battery charging is defined by the duty cycle which is determined through complex soft computing techniques (Zongo, 2021; Bahri and Harrag, 2021; Ahmed et al., 2021).

The MPPT controllers are classified into three categories based on control and optimization principles (Mao et al., 2020). The first one is the classical techniques, modern intelligent control, and array reconfiguration schemes. Conventional techniques such as Perturb and Observe (P&O), incremental conductance, hill climbing, modified incremental conductance, hybrid incremental conductance have been seen to perform well only with uniform irradiance and are unable to find the Global Maximum Power Point (GMPP) (Feroz Mirza et al., 2020). These gradient-based algorithms operate at a single point in the search space. The only comparison is made between consecutive samples of power magnitude between current and previous sample ($\Delta P = P_{new}(k) - P_{old}(k-1)$). The change in power is utilized for the decision-making process. Since the algorithms utilize the change in duty cycle (P&O) or change in conductance (IC) to improvise the output power, therefore, the updated control signal (D) forces to move in only one direction at a time. PS generates multiple epic points (maxima) where the gradient slop equals zero. At these points of operation, oscillations are observed by classical techniques. The magnitude of such oscillation is directly proportional to the step size of the control signal. To quickly attain MPP large step size is useful however under PS this generates undesired oscillations caused by power loss in steady-state. To reduce such power loss smaller step size is preferable. But this leads to slower tracking. Hence a balanced approach is needed. Adaptive control techniques are utilized to modify the step size to take advantage of quick and simple implantation. Up to 90% reduction in oscillation is achievable around MPP. But the PS problem remains unresolved. As a solution, swarm intelligence (SI) based metaheuristic algorithms are utilized. These algorithms initialize multiple random solutions and using an objective function such as power ($max(P_{i-n})$) or ref voltage improvised the solution over iterative time. Therefore meta-heuristic optimization techniques have been studied in the literature. Direct online control of the base system is possible under this scenario. These techniques are implemented as MPPT control for actively tracking GMPP. The meta-heuristic optimization techniques are Particle Swarm Optimization (PSO), Salp swarm optimization (SSO), Harris hawk optimization (HHO), Flashing Fireflies Optimization (FFO), Grey

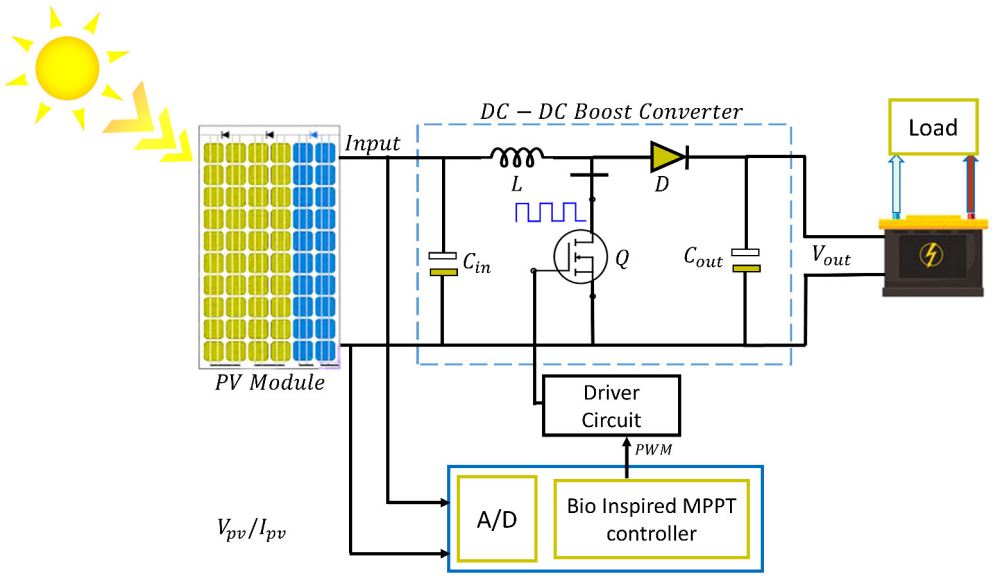

Fig. 1. PV system interfaced with load through boost converter.

Wolf Optimization (GWO), Group teaching optimization algorithm (GTOA), Cuckoo Search (CS), PSO-gravitational search (PSO-GS), Bat optimization algorithm (BOA), Grasshopper optimization (DFO), Henry gas solubility optimization, Artificial Bee Colony (ABC), Dragonfly Optimization (DFO), improved team game optimization, Squirrel Search Optimization Algorithm (SSA) (Fares et al., 2021), and Pigeon Optimization Algorithm (POA) (Mirza et al., 2020b,a; Mansoor et al., 2020b,a; Mirza et al., 2019; Javed et al., 2019). The reconfiguration techniques utilize switching modules to minimize the effects of partially shaded modules. These schemes utilize series, parallel, total cross-tied, series–parallel, Honeycomb, and Bridge link configurations. The performance of metaheuristics is highly dependent upon factors such as parameter tuning, population size, objective function, fitness function, and position updating mathematical models (Shams et al., 2020). The efficiency of the information-sharing model and the extent of randomness in the searching process. Levy flight function utilized by the HHO, DFO, and CS generates highly random fluctuations and random intervals caused by the sigma factor(σ). Modified Butterfly optimization (Shams et al., 2020) makes use of V_{oc} dependent tuning parameter. The pheromones decay factor of ACO and probability function for random solutions generate undesired large surges in voltage. The movement of particles in ABC restricted by parameter 'a' decreases with iterations causing slower convergence towards the optimum solution. In recent years neural networks (NN) are employed in combination with fuzzy logic control. The membership functions of the hybrid Neuro-Fuzzy parameters structure are updated using an enhanced mechanism that allows for the adaptive response in steady and dynamic tracking stages undercharging operating conditions.

PSO is a representative member of SI. The random numbers embedded in velocity vectors embed oscillations. The movement of the swarm particles dependent upon the P_{best} and G_{best} which are personal best and global best respectively. DFO takes large iterations to track GM because of the parameter 'c'. The movement of particles in PSOGS is restricted due to the gravitational effect which causes the PSOGS to fall into the LM trap. So, high tracking and settling time, the oscillations at GMPP, falling into LM trap, and low tracking efficiency are the drawbacks of techniques described above (Chandrasekaran et al., 2020). To effectively cater to these drawbacks a metaheuristic optimization algorithm-based MPPT technique is presented in this work (Zhou et al., 2021).

Conventional MPPT techniques i.e. P&O, INC, Mod-INC show low efficiency under partial shading conditions due to trapping in local maxima, which decreases the efficiency of the PV system. Intelligent MPPT techniques or Machine learning based MPPT techniques have high efficiency but these techniques require a large amount of data for training and testing the model. In addition, these techniques are system-dependent which means we need to train and test the model again whenever the PV system changes. Swarm intelligence (SI) based MPPT techniques are the viable solution for the extraction of maximum power under partial shading conditions but high tracking time, slow convergence time, low tracking efficiency, low tracked power, and extracted energy are the drawbacks observed. Hence, novel swarm intelligence-based MPPT techniques are required to fill this gap. A literature review of various optimization techniques for MPPT of PV, TEG and hybrid PV-TEG systems is presented in Table 1.

1.2. Contributions

In this study, a stochastic based Dynamic Group Cooperative Optimization Algorithm (DGBCOA) is advocated as a tool to discover the GMPP of SPV Panels. The control is attained by varying the duty cycle of the DC boost converter. The MPPT control is mathematically modeled to minimize the drawback of existing MPPT control techniques. Comparison is made with state of the art MPPT techniques presented in literature i.e. PSO, CS, ABC and DFO. The main contributions of the proposed work are presented below:

1. The proposed MPPT technique required few iterations to track global maxima due to the simultaneous working of explorative and exploitative groups.
2. The proposed technique has only 1 tuning parameter which makes it less difficult to balance the searching mechanism.
3. DGBCO based control technique for MPPT can also track GMPP under PSC and dynamic PS conditions with high efficiency.
4. Due to lower complexity of proposed algorithm, it can be implemented on a very low-cost microcontroller for experimental validation.
5. The results of four cases validate the dominance of the presented MPPT technique.

Table 1
Comparison of various MPPT techniques.

Reference	Technique	Summary
Immad Shams, et al.	Modified Butterfly Optimization Algorithm (BOA)	In this research work, a modified Butterfly Search Algorithm for MPPT was proposed which was capable of differentiating between partial shading, uniform shading and load variations. Experimental results proved that the method provided a tracking efficiency of 99.85%.
Dalila Fares, et al.	Improved Squirrel Search Algorithm (ISSA)	A novel MPPT technique was used in this research based upon the Improved Squirrel Search Algorithm to track global maximum power point (GMPP). The efficiency and average tracking time were 99.48% and 0.06 s respectively. This technique reduced track time 50% as compared to conventional Squirrel Search Algorithm (SSA).
Kok Soon Tey, et al.	Differential Evolution Algorithm	In order to track global maximum power point (GMPP), an improved differential Evolution Algorithm was proposed which provide quicker response against load variations. The response time of this algorithm was 0.1 s to load variations and it tracked GMPP with an accuracy of 99%.
Houssam Deboucha, et al.	Collaborative swarm algorithm (CSA)	Collaborative swarm algorithm (CSA) algorithm-based MPPT methodology was applied to the PV system in the presence of PSC. Simple structure with only two tuning parameters, high efficiency and fast-tracking were some of the merits of the CSA algorithm. Experimental results showed 99.8% efficiency under PSC with a tracking time of up to 0.68 s.
Bo Yang, et al.	Adaptive compass search (ACS)	In this work, a single agent-based Adaptive compass search (ACS) was utilized for MPPT of the TEG system under heterogeneous temperature difference conditions. Less computational cost, high energy generation (513.89% more than P&O) and small power variations were some of the merits of the ACS algorithm

Table 2
Characteristic of PV panel: "Clean Source & Energy CSE115M-1".

Parameter	Value
Optimal power point, P_{mpp}	114.996 W
Optimal voltage, V_{mp}	25.9 V
Optimal current, I_{mp}	4.44 A
Panel short current, I_{sc}	5.09 A
Panel open voltage, V_{oc}	30.2 V
Shunt resistance R_P	57.82 Ω
Series resistance R_s	0.1041 Ω

6. Statistical analysis is carried out to check the robustness and sensitivity of proposed technique.

The rest of the paper is structured as follows: PV cell modeling and effect of partial shading on PV systems is explained in Section 2, Section 3 explains the DGBCO algorithm with implementation and working of DGBCO as MPPT control under PS condition, Extensive case study with statistical analysis and experimental validation is presented in Sections 4 and 5 contains some concluding remarks of this work.

2. Modeling of photovoltaic cell and effect of partial shading

Multiple models are presented in the literature for the estimation of PV cell parameters. The single diode PV model is a simple and efficient equivalent model. An ideal model of PV cell as shown in Fig. 2 consists of an anti-parallel diode with a current source. The current generation depends upon the intensity of light and temperature. PV model layout is presented in Fig. 2 in which series and parallel resistances are added. The mathematical model of PV is discussed in Teo et al. (2020), Anani and Ibrahim (2020) the ideal and practical mathematical formulation of the single diode model (Teo et al., 2020; Anani and Ibrahim, 2020; Humada et al., 2016; Hejri et al., 2014; Ishaque et al., 2011a). The electrical characteristics of PV array "Clean Source & Energy CSE115M-1" are shown in Table 2 that has been modeled in this study.

Effect of Partial Shading on I–V/P–V Curve

To meet the increasing demand of energy, high power generation is required by combination of multiple PV panels in Series–Parallel combination. Under uniform irradiance and temperature

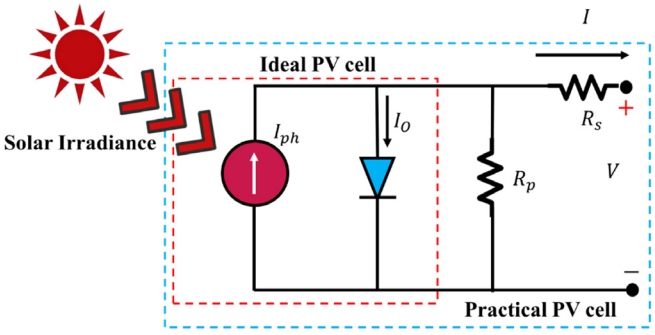

Fig. 2. Model of PV cell (single diode).

on all panels gives rise to only peak in I–V and P–V curves as shown in Fig. 4(b). This peak is the maximum power point (MPP) and PV panels need to be operating at this point if maximum power is required. However, environmental conditions are not always uniform. This nonuniformity in irradiance and temperature can occur due to nearby buildings, trees, dirt, or clouds shadow as presented in Fig. 3 (Anon, 2021, 2020; Ishaque et al., 2011b; Srivastava et al., 2020). Unlike, uniform conditions, there exist multiple peaks in P–V and I–V curves as shown in Fig. 4(a) for non uniform conditions. This shows a single global maximum point and multiple local maximum points. This GMPP could be left-skewed, right-skewed, or consolidated in the middle. These cases are presented in results and discussion Section 4. Therefore, a sophisticated technique is required to track this GMPP under all dynamic conditions with high efficiency (Yadav et al., 2020; Tey et al., 2018).

3. Proposed technique

DGBCO is a meta-heuristic population-based algorithm that imitates the cooperation between the individuals in the swarm to obtain a global solution of the engineering optimization problem. Logically, persons tend to live in communities and groups and usually, they gather food and fight against the enemy together by exchanging their roles when achieving tasks (Fouad et al., 2020).

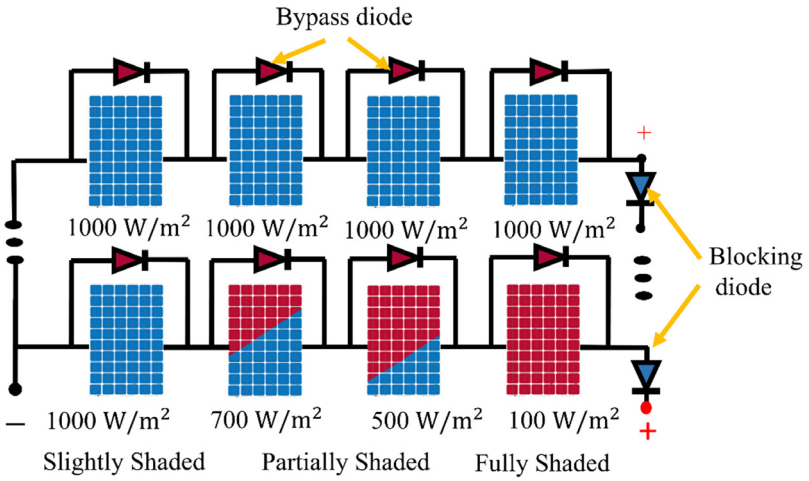

Fig. 3. Regular and irregular shading patterns on PV modules.

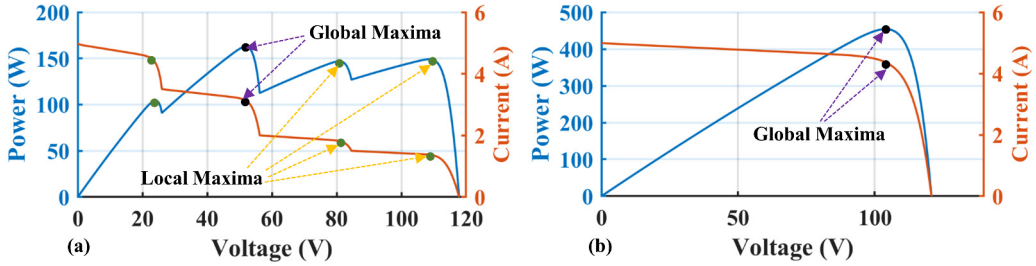

Fig. 4. (a) I–V and P–V curves under PS condition. (b) I–V and P–V curve under uniform shading.

As presented in the literature, the results of the engineering optimization problem contain the completion of two tasks. Exploration and exploitation phase. In other optimization algorithms, all the search agents do the exploration–exploitation phase collectively which stagnates the movement of particles over the iterations. In DGBCO, the search agents are divided into two subgroups which perform on the two complementary tasks. This behavior of DGBCO for the exploration and exploitation phase in search space preserves convergence and encourages diversity. Also, DGBCO increases the number of search agents for exploration, if the performance does not enchase three iterations consecutively. Fig. 5 provides the graphical abstract of the optimization algorithm with a position updating mechanism during search phases.

3.1. Initialization

Initialization of DGBCO starts by assigning random locations to every search agent in the search space within the range of maximum (Max_p) and minimum (Min_p) limits. The parameters required for DGBCO to start the process of optimization are:

1. Population size represents the number of solutions.
2. The dimensions of search space, number of optimization objectives, upper and lower boundary limits
3. Fitness function for each objective function.

3.2. Exploration and exploitation: Balance between two phases

DGBCO changes the number of search agents dynamically in every sub-group. Initially, DGBCO starts with a 70%–30% ratio where 70% of search agents are in the explorative phase and 30% are in the exploitive phase. Since at the start the search agents need to search the entire search space for the global optimum solution, therefore GDGBCO assigns a high number of agents at the start of the process to the explorative phase. Fig. 5 shows the number of search agents' changes in the explorative and exploitation phase in DGBCO over the iterations.

3.3. Exploration group

The explorative phase is an important part of the optimization algorithm because it is responsible for searching for promising places in search and also to avoid trapping into the local peak. DGBCO uses two techniques in the explorative phase, that is, exploration of search space in the surrounding of solution and mutation.

In the first procedure, the search agent looks for a promising solution around its position in search space. For this, DGBCO uses Eqs. (1) and (2).

$$D = r_1 \cdot (X(t) - 1) \tag{1}$$

$$X(t+1) = X(t) + D \cdot (2r_2 - 1) \tag{2}$$

where the ranges of random vectors are $r_1 \in [0, 1]$ and $r_2 \in [0, 2]$, X represents the current solution and the D is the diameter of the circle in which different agents look for better areas. The mutation is the second method implied by DGBCO. The generic operator is used to maintain the diversity in the population. This helps to avoid the local optimum preventing an early convergence. The DGBCO achieves high exploration ability due to the mutation phenomenon.

3.4. Exploitation group

In the exploitation phase, the search agents get the global best solution and converge towards the fittest solution. The exploitation group in DGBCO uses two techniques which are: converge

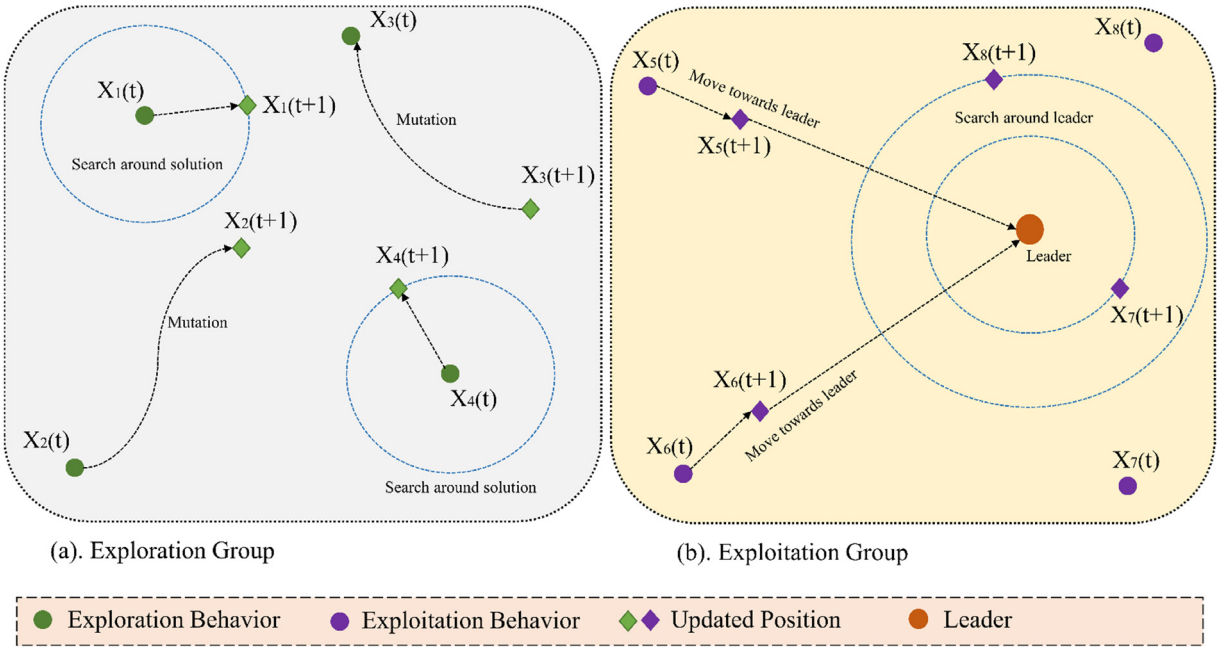

Fig. 5. Model of dynamic group-based cooperative optimization algorithm.

ring towards the global best solution and the search around the best solution. In the first technique, the search agents travel towards best solution using Eqs. (3) and (4).

$$D = r_3 \cdot (L(t) - X(t)) \tag{3}$$

$$X(t+1) = X(t) + D \tag{4}$$

where r_3 is the random number in the range [0, 2] that controls step-by-step tracking towards the global solution. L represents the best solution.

In the second phase, DGBCO uses Eq. (5) to Eq. (6) search around best solution because that is the most probable place to find a better solution.

$$D = L(t) \times (K - r_4) \tag{5}$$

$$X(t+1) = X(t) + D \cdot (2 \cdot r_5 - 1) \tag{6}$$

$$K = 2 - \frac{2 \times t^2}{(iters\_count)^2} \tag{7}$$

where r_4 and r_5 are random numbers in the interval [0, 1], K decreases its value exponentially from number 2 to 0 as the iterations pass.

3.5. Best solution's Elitism

DGBCO selects the best solution and passes it to the next iteration without any changes. This strategy improves the global search capability of the algorithm.

3.6. DGBCO's implementation as control under different operating condition

Duty cycles are initialized randomly in search space i.e. between 0 and 1. Particle's position is updated by DGBCO. Pseudo-code for DGBCO's implementation as MPPT is presented in Fig. 6. (See Fig. 7.)

For re-initialization of DGBCO, the change in power is needed to detect large change which occurs due to abrupt change in environmental conditions. The re-initialization condition is

$$if \ \frac{\left|P_{PV_{new}} - P_{PV_{old}}\right|}{P_{PV_{old}}} \geq P_{PV}(\%) \tag{8}$$

Table 3
Components specifications for simulation.

Case #	PV1	PV1	PV1	PV1	GM
Case 2	1000 W/m^2	300 W/m^2	800 W/m^2	600 W/m^2	219.6 W
Case 3	1000 W/m^2	700 W/m^2	300 W/m^2	100 W/m^2	165.5 W
Case 4	1000 W/m^2	650 W/m^2	900 W/m^2	480 W/m^2	255.5 W

P_{PV} is the panel's power. The working of DGBCO under different operating conditions is explicitly presented in flow chart as shown below.

3.7. Tracking procedure of DGBCO as MPPT control

In this section working principle of DGBCO as MPPT is explained briefly. Fig. 8 shows the complete tracking procedure of GMPP under PSC by DGBCO control. As presented in Fig. 8(b), four duty cycles are initialized randomly on PV curve i.e. search space. After initialization, DGBCO updates the position of particles after evaluating the fitness of every particle and passing on the information of best particle to each other. Due to working of both exploration and exploitation groups in the search of global maxima gives excellent LM trap braking capability to DGBCO MPPT control. High exploration capability of DGBCO can be verified by the fluctuations of voltage in Fig. 8(c) and power in Fig. (a) In initial stages i.e. time less than 0.25 s. After tracking and settling at GMPP under less than 0.3 s, DGBCO control shows zero oscillations which causes very low power loss.

4. Case studies: Discussion

To gauge the performance of the proposed DGBCO based MPPT technique multiple case studies are presented. Case 1–4 utilize a PV system in 4 × 1 configuration with total capacity of 0.459984 kW. Fast varying condition is particularized in Case 1. Three different PS scenarios are presented in Case 2, Case 3, and Case 4. To authenticate the performance in real time application, experimental validation is presented in Case 5. Table 3 provides the specifications for experimental simulations.

```
input parameters (size of population, iteration count)
initialize population d=[d1, d2, d3, ..., dn]
    while(t<iters_max)
        evaluate fitness of every energy particle, select the best solution
        K=2-2× t/iter_max
        update particles number's in every group
        if the global best solution doesn't alter from the prior 2 iterations
            increase the particles number's in exploration group
        end if
        for every solution in exploration group
            update the value of r1, r2 and P
            find global best solution by applying elitism
            if P≥0.5
                apply mutation on the solution
            else
                keep searching around current solution using Eq. (2)
            end if
        end for
        for every solution in exploitation group
            find global best solution by applying elitism
            update the value r2, r3, r4, and P
            if P≥0.5
                update positon in direction of best solution using Eq. (3) and
            Eq. (10)
            else
                keep searching around best solution by Eq. (5) – Eq. (7)
            end if
        end for
        update solution that goes beyond limit.
        update prev_fitness_1, prev_fitness_2
    end while
Return dbest
```

Fig. 6. Pseudocode of DGBCO for MPPT control.

5. Fast changing irradiance: Case 1

Case 1 is presented to view the sensitivity and robustness of the control technique against quick shifting of irradiance magnitude across all panels in series connection. Irradiance level alters every 2 s and the levels are presented in Fig. 9. As depicted in Fig. 9. at STC, the power is 459.96 W which changes to 288.10 W after 2 s and again changes to 389 W at 4 s. At STC, the power tracked by DGBCO is 459.3 W which is highest in comparison to DFO, ABC, CS, and PSO. Power tracked by DFO is 458.7 W, ABC 458.5 W, CS 458.45 W, and PSO 458.3 W. DGBCO achieves the highest efficiency of 99.86% followed by DFO's 99.72%, DFO's 99.68%, ABC's 99.67%, and PSO's 99.63%.

Since, random numbers are present in the velocity vector of PSO used for position update, large oscillations can be witnessed at the GM. Similarly, CS and ABC also show oscillations after achieving GM. Male female dynamic grouping in DFO makes it slow to converge to GM. Although DFO achieves reasonable efficiency. However, oscillations result in significant power loss. At STC, the tracking time of DGBCO, DFO, ABC, CS, and PSO is 0.412 s, 0.604 s, 0.550 s, 0.705 s, and 0.961 s respectively. Fig. 10(a) and Fig. 10(b) display the tracked power in case I. The robustness of DGBCO MPPT can be observed by the effective re-initialization of particles and tracking of GM under fast varying irradiance. The duty cycle and its details are given in Figs. 10(c) and 10(d), respectively.

To effectively measure the tracking performance of all techniques under Case 1, average power tracked is an effective tool. The average power for Case 1 is 379.02 W. The superior performance of DGBCO MPPT control can be observed since the average power tracked by DGBCO is 378.1 W is the highest. Average power traced by DFO is 377.23 W, ABC is 376.83 W, CS is 376.7 W, and PSO is 376.76 W. The efficiency attained by DGBCO, DFO, ABC, CS, and PSO is 99.75%, 99.52%, 99.42%, 99.38%, and 99.40% respectively. The energy comparison is depicted in Fig. 15 which also validates that DGBCO extracts the higher energy in comparison with competing MPPT techniques.

6. PSC-A: Case 2

Case 2 deals with PSC-A in which GM is located at the center of local peaks as shown in Fig. 11. The GM is at 219.6 W and the local peaks are at 103.8 W, 184.7 W, and 151.2 W respectively. To effectively track the GM in PSC-A, the MPPT techniques need to be effective in LM trap breaking which will lead to all the population converging at GM. Power traced by DGBCO, DFO, ABC, CS, and PSO is 219. 3 W, 218.9 W, 218.5 W, 218.1 W, and 217.9 W. The efficiency attained by DGBCO, DFO, ABC, CS, and PSO is 99.86%, 99.68%, 99.49%, 99.31%, and 99.21% respectively. Fig. 17 and Fig. 18 provide the comparison of tracked and zoomed-in tracked power which states that DGBCO is effective in tracking GM and shows minimum oscillations at GM. (See Fig. 19.)

The tracking time of DGBCO, DFO, ABC, CS, and PSO is 0.321 s, 0.510 s, 0.561 s, 0.681 s, and 0.821 s respectively. Evidently, less time is taken by DGBCO for tracking and settling at GM in comparison with competing MPPT techniques as shown in Figs. 12(c) and 12(d) in terms of control signal iterative behavior.

7. PSC-B: Case 3

Case 3 deals with PSC-B in which GM is also located at the center as depicted in Fig. 13 The value of power at GM is 165.5 W.

Figs. 14(a) and 14(b) shows the comparison of tracked and zoomed-in tracked power and the power traced by DGBCO, DFO,

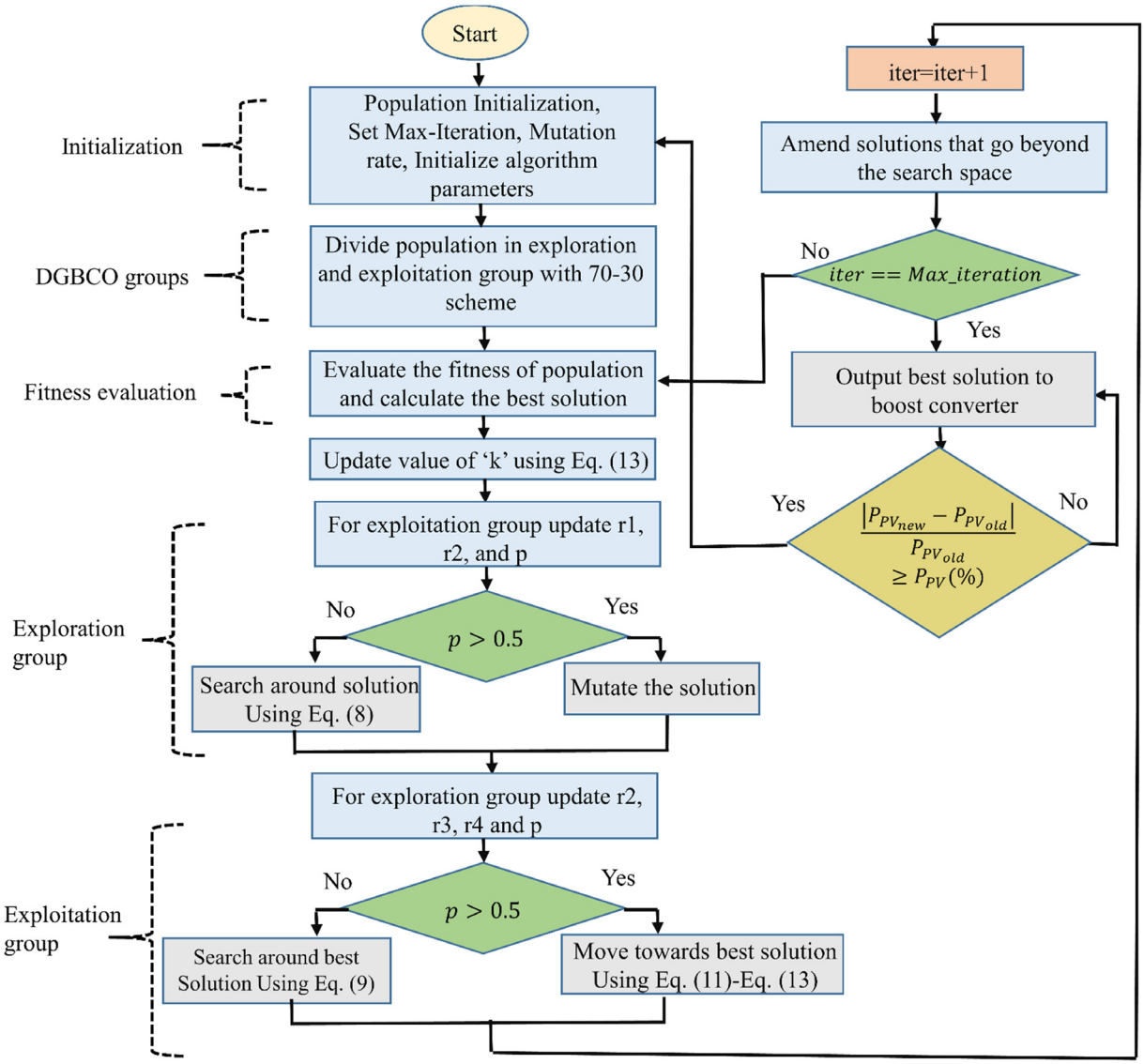

Fig. 7. Flow diagram for DGBCO's implementation as MPPT control.

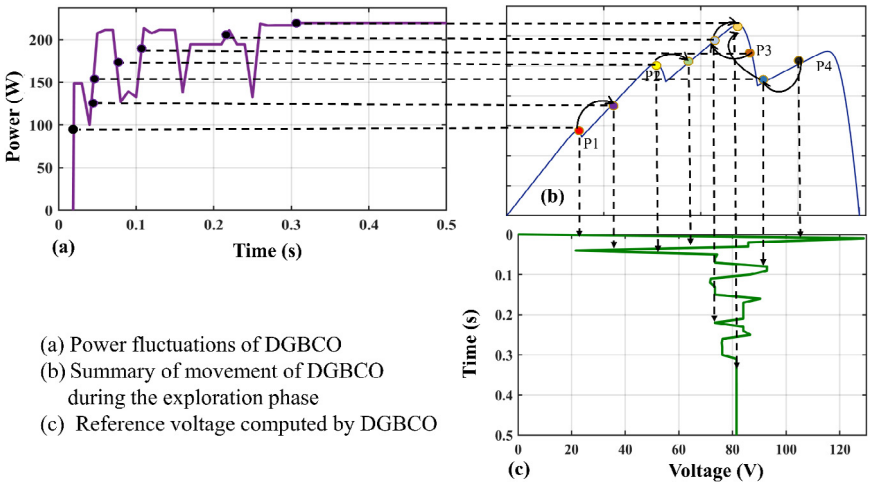

(a) Power fluctuations of DGBCO
(b) Summary of movement of DGBCO during the exploration phase
(c) Reference voltage computed by DGBCO

Fig. 8. Tracking arrangement of DGBCO under PS condition.

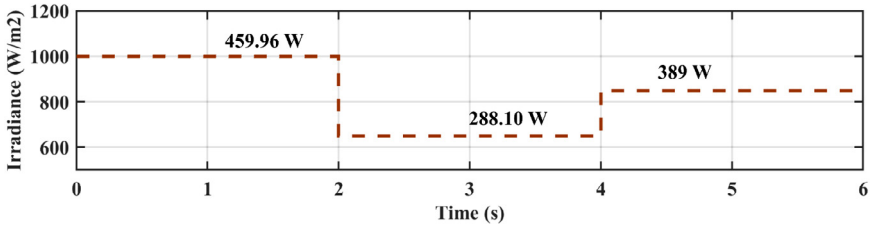

Fig. 9. Irradiance variation with the maximum power at that irradiance level.

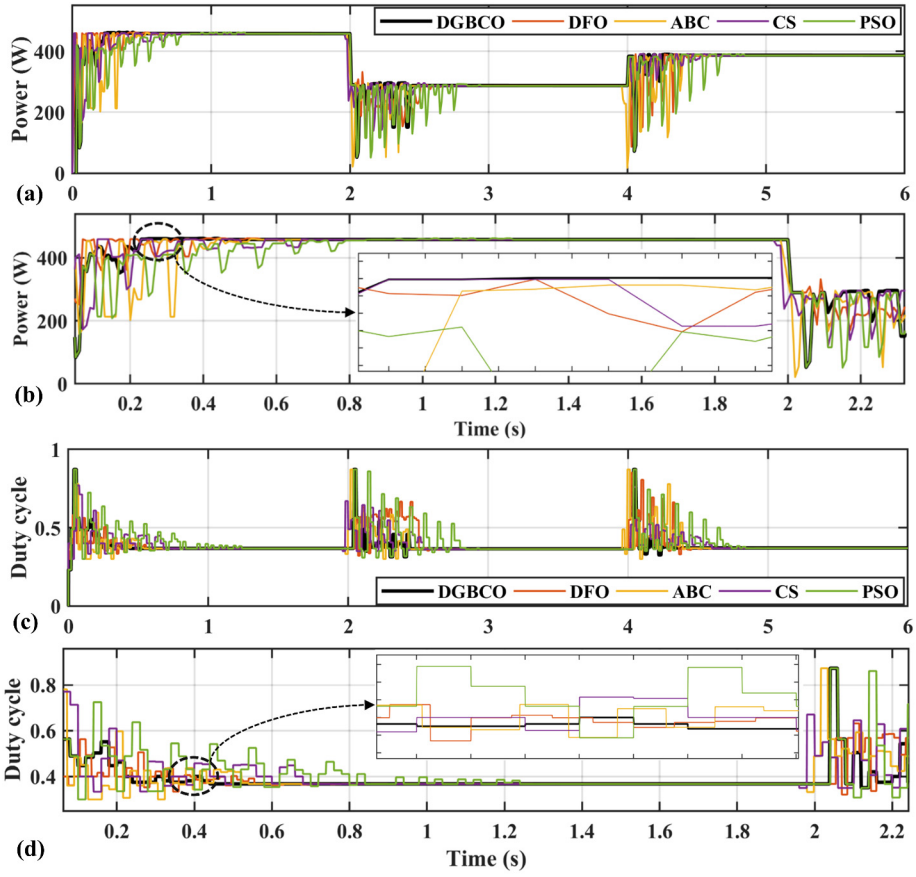

Fig. 10. (a) Tracked power in Case 1. (b) Zoom view of tracked power. (c) Duty cycle fluctuations in Case 1. (d) Zoom view of duty cycle.

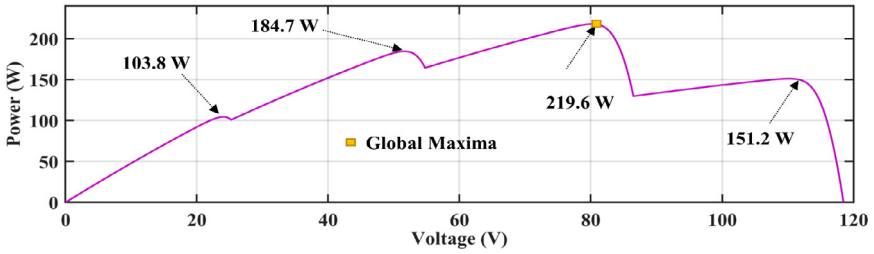

Fig. 11. PV curve for PSC-A condition.

ABC, CS and PSO is 165.3 W, 165.1 W, 165 W, 164.4 W, and 164.2 W with an efficiency of 99.87%, 99.75%, 99.69%, 99.33%, and 99.21% respectively. The excellent LM trap breaking capability of DGBCO can be seen in Figs. 14(c) and 14(d).

Due to up-gradation of particle position using P_{best} and G_{best} in PSO, large oscillations are observed. The movement of ABC particles is restricted over the iterations that make it settle at a lower magnitude. DGBCO has explorative and exploitation groups searching together which makes the DGBCO MPPT control track and settle at GM more efficiently. The tracking time of DGBCO, DFO, ABC, CS, and PSO is 0.340 s, 0.462 s, 0.541 s, 0.690 s, and 0.805 s respectively.

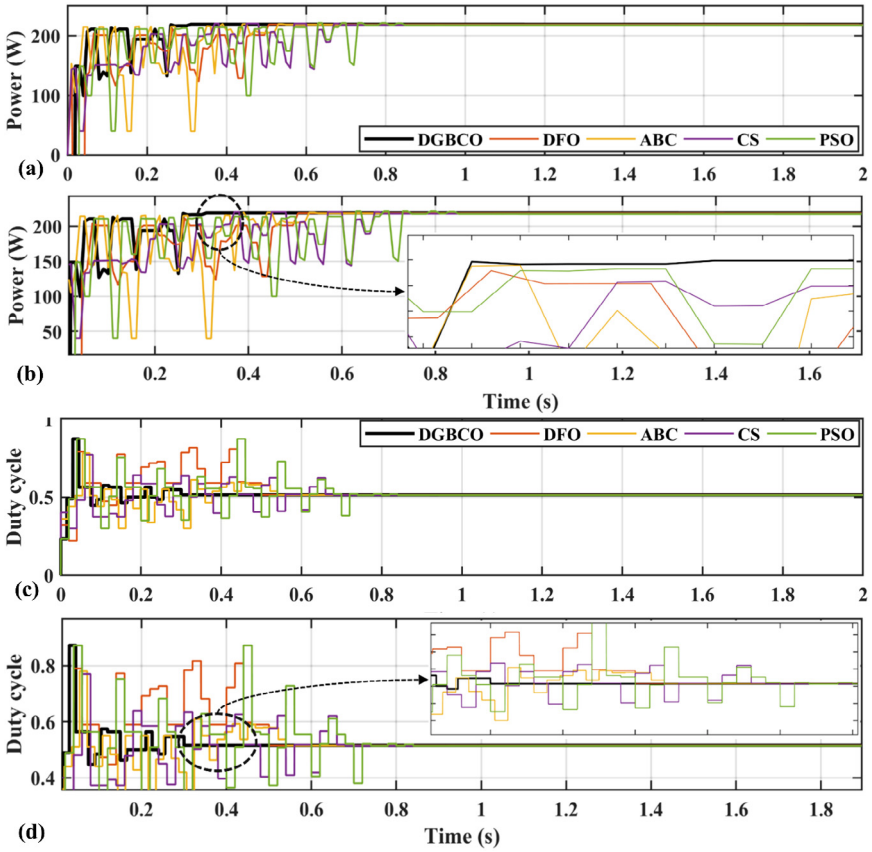

Fig. 12. (a) Tracked power in Case 2. (b) Zoom view of tracked power. (c) Duty cycle fluctuations in Case 2. (d) Zoom view of duty cycle.

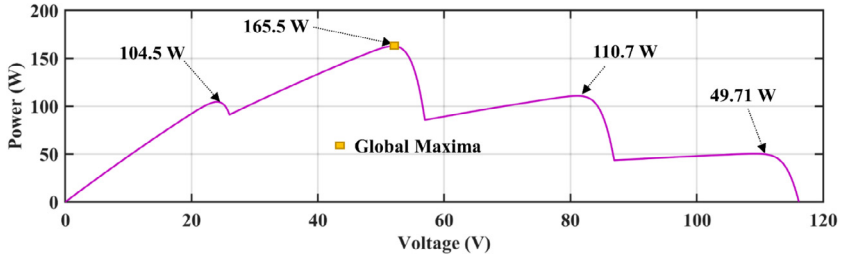

Fig. 13. PV curve for PSC-B.

8. PSC-C: Case 4

Case 4 deals with PSC-C in which LM and GM have a very small difference of power as depicted in Fig. 15. GM is located at 244.5 Wl and LM is located at 241.5 W. This case is presented to compare the LM trap-breaking capability of compared techniques.

The power traced comparison and zoomed power comparison of power tracked is presented in Figs. 16(a) and 16(b) respectively which states that PSO and CS fall into the LM trap and settle at LM by DFO and ABC shows promising LM breaking capabilities. DFO and ABC settle at a lesser value than GM. However, DGBCO shows excellent capability in breaking LM and settling at GM.

Power traced by DGBCO, DFO, ABC, CS, and PSO is 244.3 W, 244.1 W, 243.8 W, 240.9 W, and 240.8 W with an efficiency of 99.91%, 99.83%, 99.71%, 98.52%, and 98.48% respectively. The GM tracking time is 0.461 s, by DGBCO followed by DFO 0.612 s, ABC 0.642 s, CS 0.705 s, and PSO is 0.760 s. Figs. 16(c) and 16(d) show the control signal duty cycle comparison.

9. MPPT rating

In this section, a rating system is presented to numerically rate the performance of the competing techniques similar to Fouad et al. (2020). As per Eq. (15) seven factors are chosen to devise the grading criteria. Namely average efficiency, number of random numbers, average tracking time, modification required in hardware for implementation, number of tuning parameters, the requirement of the maximum number of iterations (iter_max) to obtain termination criteria, and lastly the response of variation in irradiance. The rating is average is calculated using Eq. (9) as

$$MPPT\_rating = \frac{Total\ achieved\ rating}{7} \tag{9}$$

Table 4 summarizes the score of each technique across every grading factor. The rating 1–4 indicates the score from the best to the worst.

For the efficiency factor, the values between 99.5%–100% score 1, for the range 99%–99.5% score is 2, 98.5%–99% is 3 and for the

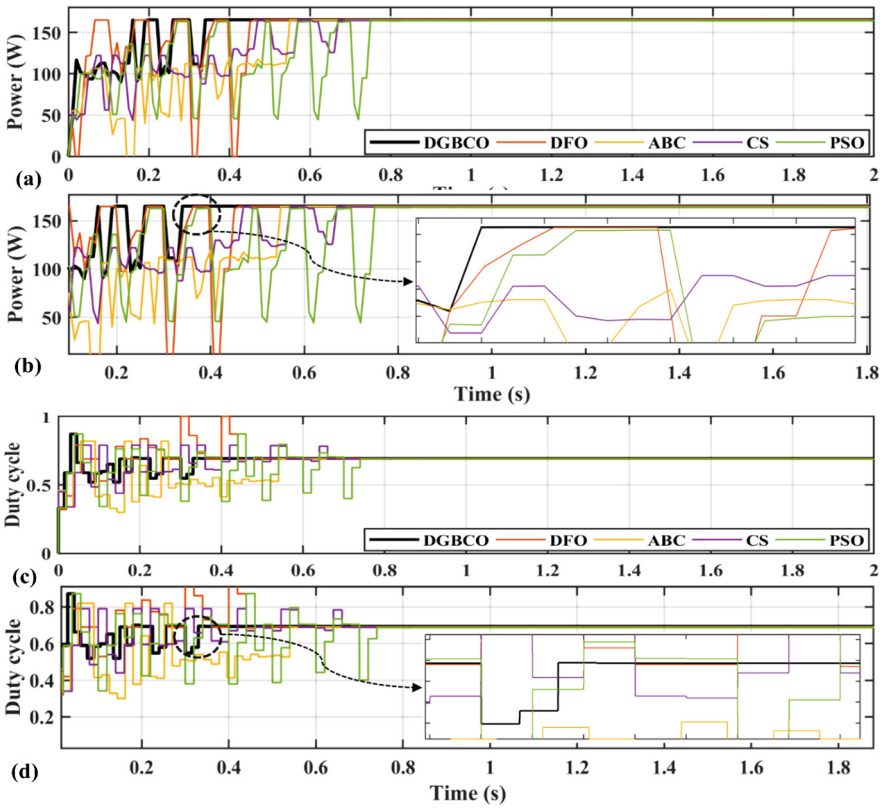

Fig. 14. (a) Tracked power in Case 3. (b) Zoom view of tracked power. (c) Duty cycle fluctuations in Case 3. (d) Zoom view of duty cycle.

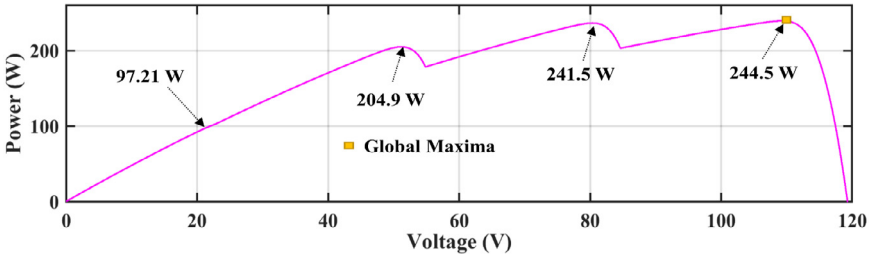

Fig. 15. PV curve of PSC-C condition.

Table 4
Components specifications for simulation.

Component	Value
Photo voltaic panel/Module max power	114.996 W
Inductance, (L)	1.39 mH
Input capacitance, (Cin)	18 uF
Output capacitance, (Cout)	520 uF
Switching frequency of FET, (f)	50 kHz
Load resistance	70 Ω

efficiency of less than 98.5%, the rating is kept 4. For the number of tuning parameters in an algorithm, the rating is 1 if a single parameter is tuned, for two tuning parameter rating score is 2, for three tuning parameters it is 3. The score is kept at 4 for four and above tuning parameters. The random numbers although slow the convergence but are essential to locate the GM and maximize the exploration of the search space. Additionally they are essential for breaking local solutions. Therefore the rating is 1 if no random numbers are required. for one random numbers rating is 2 and so on. The random variables rating is 4 for number $\geq$3. If the termination criteria are not met prior to iter_max is achieved the score is 4 if it is not, then the rating is 1. For the average tracking time the rating is 1 between 0 and 500 ms. 2 between 500 and 750 ms, 3 between 750 and 1000 ms and 4 for average tracking time of 1000 ms and above.

For the irradiance variation factor, the rating would be 1 if the response is less than 0.25 s, it is 2 between 0.25 s and .5 s, 3 between 0.5 s and .75 s, and for more than 0.75 s, the rating would be 4. If hardware modification is required in the existing hardware to accommodate the MPPT control for the implementation of MPPT then the rating would be 2 and score is 1 if no modification is required.

Table 4 shows the best MPPT rating of 1.571 is achieved by DGBCO proposing superior performance in technical and non-technical aspects. DGBCO is easy to implement due to its simple structure and only one tuning parameter.

10. Experimental validation: Case 5

This case is presented which experimentally authenticate performance of presented technique. Boost converter which is acting as an interface between PV emulator and Load. The MPPT technique is used to generate duty cycle which is fed to boost converter. PV current and voltage through sensors is fed to the

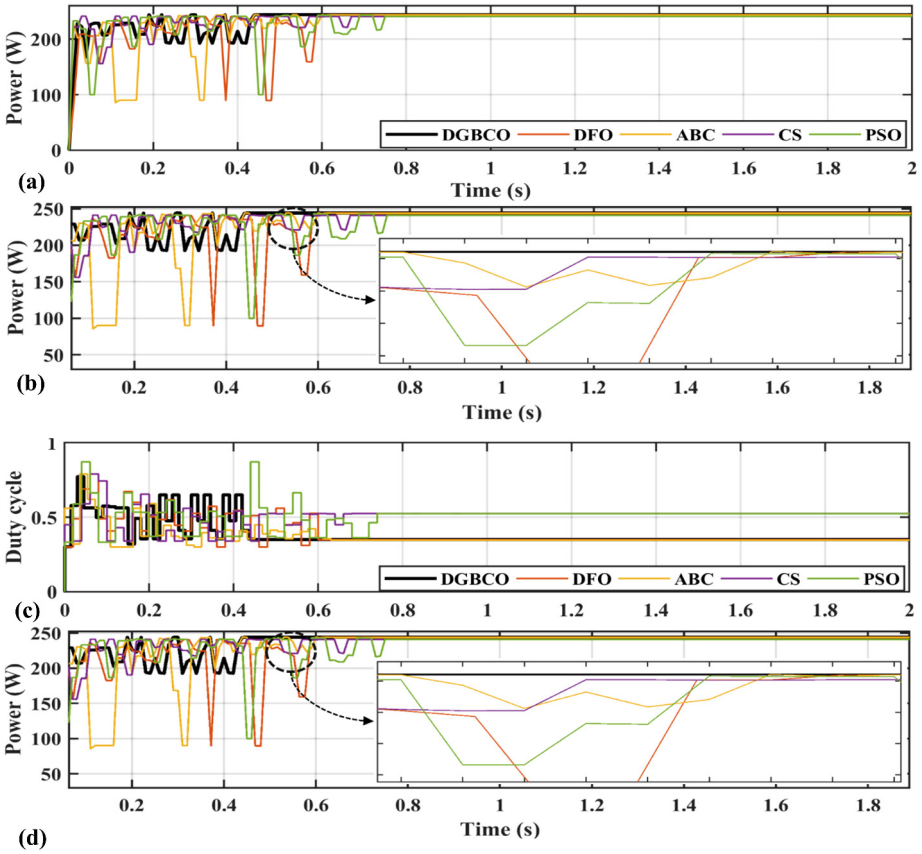

Fig. 16. (a) Tracked power in Case 4. (b) Zoom view of tracked power. (c) Duty cycle fluctuations in Case 4. (d) Zoom view of duty cycle.

Table 5
MPPT rating comparison of competing techniques with DGBCO.

Tech. name	Average efficiency (%)	Average tracking time (s)	Termination criteria achieved	Modification in hardware	No. of tuning parameters	No. of random numbers	Response time in irradiance variation (s)	MPPT rating
DGBCO	99.88 (1)	0.3835 (1)	No (1)	No (1)	1 (1)	5 (4)	Fast (2)	1.571
DFO	99.74 (1)	0.5470 (2)	Yes (2)	Yes (2)	3 (3)	1 (1)	Very slow (4)	2.142
CS	99.45 (2)	0.6952 (2)	No (1)	No (1)	1 (1)	2 (3)	Slow (3)	1.857
PSO	99.38 (2)	0.8360 (2)	No (1)	No (1)	3 (3)	2 (3)	Very slow (4)	2.285
ABC	99.64 (1)	0.5735 (2)	Yes (2)	No (1)	1 (1)	2 (3)	Slow (3)	1.857

Table 6
Technical specs of PV panel "HQRP 20 W Monocrystalline".

Component	Value
Optimal power point, P_{mp}	20 W
Optimal voltage, V_{mp}	17.2 V
Optimal current, I_{mp}	1.17 A
Panel short current, I_{sc}	1.31 A
Panel open voltage, V_{oc}	21.6 V

Table 7
Components used for experimental setup.

Component	Value
PV panel module	HQRP 20 W
Inductance, (L)	1.4 mH
Input side capacitance, (Cin)	10 uF
Output side capacitance, (Cout)	1200 uF
Switching frequency of FET, (f)	50 kHz
Load resistance, (R_L)	70 Ω
Voltage sensing device	B25
Current sensing device	Current module
MPPT controller	ATmega 2560
MOSFET switch	IRF730

MPPT control technique. Fig. 17 is presented which is the experimental setup implemented for testing of proposed MPPT control technique. Specifications of photovoltaic panel used for experimental setup are presented in Tables 5 and 6 shows the details of components used. MATLAB is used for data acquisition by interfacing ATmega 328 with Personal Computer.

Fig. 18(a) presented is power traced by PSO MPPT technique which shows that PSO takes 310 ms to track GMPP and 460 ms to settle. After tracking of GMPP, it is observed that oscillations exist in Fig. 18(b), which shows the zoomed view of power transients by PSO. The average power tracked by PSO is 14.2 W. As compared to PSO, DGBCO tracks the GM in 170 ms and settles at GM in 250 ms. Figs. 18(c) and 18(d) show the power traced by DGBCO and zoomed-in traced power, respectively. The average power tracked by the DGBCO is 14.9 W which is higher than PSO. It validates that DGBCO achieve greater than 99% efficiency, with less tracking time and settling time. The proposed technique shows very few oscillations at GMPP which causes lower power loss. Table 7 gives the results comparison summary (see Table 8).

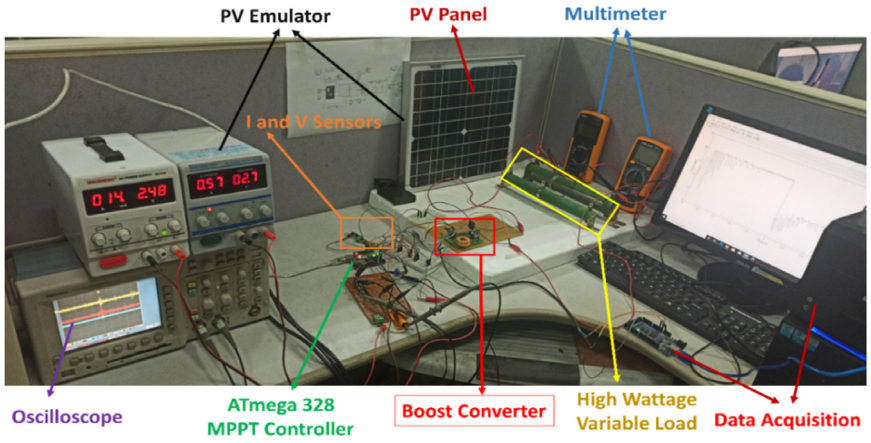

Fig. 17. Experimental setup.

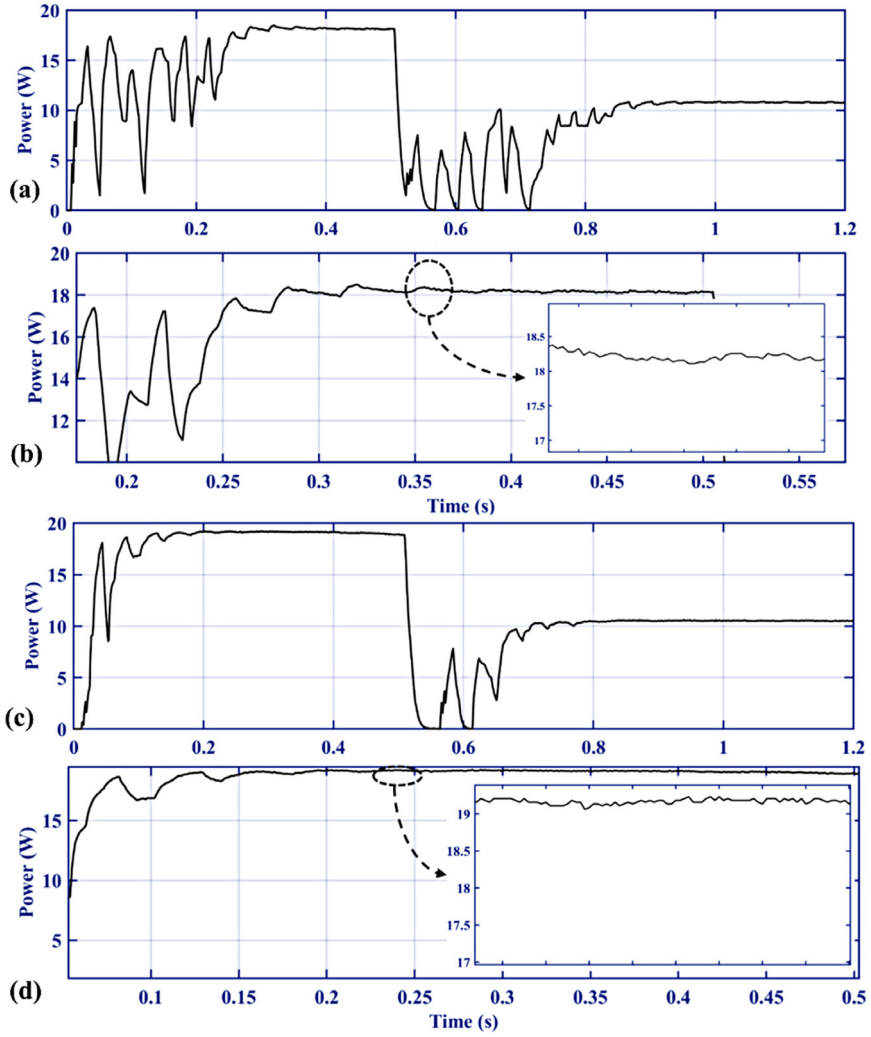

Fig. 18. (a) Tracked power by PSO. (b) Zoom view of tracked power by PSO. (c) Tracked power by DGBCO. (d) Zoom view of tracked power by DGBCO.

Statistical Analysis

The important parameters to measure the performance of MPPT techniques are Relative Error (RE), Mean Absolute Error, and Root Mean Square Error (RMSE). This statistical analysis can be done by using the equations presented below (Li et al., 2020).

$$Error_{RE} = \frac{\sum_{i=1}^{n} \left(P_{pvi} - P_{pv}\right)}{P_{pv}} * 100\% \tag{10}$$

Table 8
Quantitative comparison summary of results.

Technique	Case	Tracking time (s)	Power at GMPP	Tracked power (W)	Energy (J)	Effe. (%)
DGBCO	Case 1	0.412	459.96	459.3	2198	99.86
	Case 2	0.321	219.6	219.3	406.2	99.86
	Case 3	0.340	165.5	165.3	308.5	99.87
	Case 4	0.461	244.5	244.3	467.1	99.91
DFO	Case 1	0.604	459.96	458.7	2184	99.72
	Case 2	0.510	219.6	218.9	377.2	99.68
	Case 3	0.462	165.5	165.1	302	99.75
	Case 4	0.612	244.5	244.1	457.1	99.83
ABC	Case 1	0.550	459.96	458.5	2171	99.68
	Case 2	0.561	219.6	218.5	401	99.49
	Case 3	0.541	165.5	165	278.2	99.69
	Case 4	0.642	244.5	243.8	454.2	99.71
CS	Case 1	0.705	459.96	458.45	2153	99.67
	Case 2	0.681	219.6	218.1	400.5	99.31
	Case 3	0.690	165.5	164.4	289	99.33
	Case 4	0.705	244.5	240.9	450.1	98.52
PSO	Case 1	0.961	459.96	458.3	2114	99.63
	Case 2	0.821	219.6	217.9	378.6	99.22
	Case 3	0.805	165.5	164.2	280.7	99.21
	Case 4	0.760	244.5	240.8	448.6	98.48

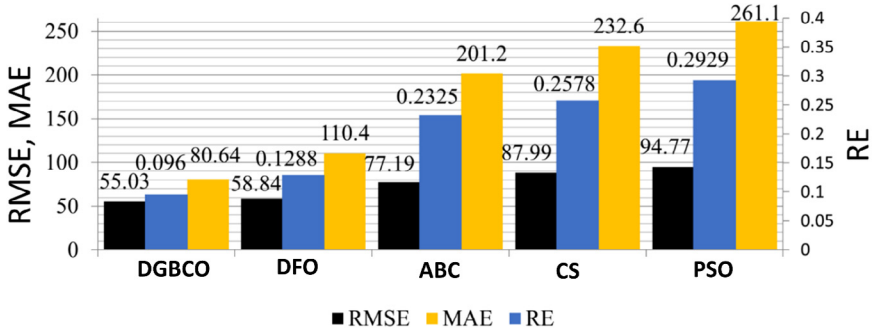

Fig. 19. Comparison of RMSE, MAE, RE.

$$Error_{MAE} = \frac{\sum_{i=1}^{n} \left(P_{pvi} - P_{pv}\right)}{n} \tag{11}$$

$$Error_{RMSE} = \sqrt{\frac{\sum_{i=1}^{n} \left(P_{pvi} - P_{pv}\right)^2}{n}} \tag{12}$$

where P_{pvi} represent power at STC, the P_{pv} is the power tracked and the n represent the number of samples. The calculated values for all the techniques are presented in Fig. 42. The analysis shows that DGBCO achieves RMSE 55.03 which is less than all other MPPT techniques. Also, the MAE and RE achieved by the DGBCO MPPT technique are far less than other techniques which validate that the proposed technique track the GMPP with high efficiency.

11. Conclusion

In this article, DGBCO has been presented as an effective controller for PV systems under partial shading conditions. Advantages of the proposed technique are higher power tracking efficiency, least fluctuation, and low oscillations at Global Maxima as compared to intelligent control techniques. Unlike existing SI-based MPPT controllers a dynamic group-based strategy is employed. This scheme allows the position updating mechanism to abandon less accurate solutions without large surges in voltage transients. Due to lesser computation time requirement and faster recovery of the optimum solution, the DGBCO achieves higher average power in lesser tracking time. The outstanding global maxima identification and tracking and balance between exploration and exploitation enable GM tracking in the least iterative time As compared to DFO, ABC, PSO, and CS The results indicated on average the DGBCOA tracks the GM within 320–461 ms achieving 30%–60% quicker GM tracking time. In addition to the improved time constraints such as tracking settling and iterative time, the power fluctuations are also significantly improvised using a search and skip algorithm that reduces the computation in the already explored region of search space. The oscillations are reduced to 0.98 W achieving a 94% reduction as compared to CS and achieving 1%–8% higher average power in the initial exploration phase. The effective and low-cost application of the proposed MPPT battery charging controller based upon DGBCOA enables the implementation in real-world applications such as PV systems, thermoelectric generation, and heat recovery operation in domestic and small scale industrial applications enabling the feasibility of cleaner renewable power generation applications.

In the future, the short-term energy forecasting modeling will be studied for PV, wind, and concentrated thermal TEG for improved high voltage-DC (HVDC) grid-connected operations.

CRediT authorship contribution statement

Syed Kumayl Raza Moosavi: Data curation, Software. **Majad Mansoor:** Funding acquisition, Resources. **Muhammad Hamza Zafar:** Conceptualization, Methodology, Supervision, Resources, Project administration. **Noman Mujeeb Khan:** Validation, Data curation. **Adeel Feroz Mirza:** Conceptualization, Formal analysis, Investigation. **Naureen Akhtar:** Visualization, Data curation, Project administration.

Declaration of competing interest

The authors declare that they have no known competing financial interests or personal relationships that could have appeared to influence the work reported in this paper.

Data availability

The data that has been used is confidential.

References

Agyekum, E.B., 2021. Techno-economic comparative analysis of solar photovoltaic power systems with and without storage systems in three different climatic regions, Ghana. Sustain. Energy Technol. Assess. 43, 100906.

Ahmed, M.M., Hassanien, W.S., Enany, M.A., 2021. Modeling and evaluation of SC MPPT controllers for PVWPS based on DC motor. Energy Rep. 7, 6044–6053.

Anani, N., Ibrahim, H., 2020. Adjusting the single-diode model parameters of a photovoltaic module with irradiance and temperature. Energies 13 (12), 3226.

Anon, 2020. Analysis of long-term performance and reliability of PV modules under tropical climatic conditions in sub-Saharan. Renew. Energy 162, 285–295.

Anon, 2021. Experimental comparative study of photovoltaic models for uniform and partially shading conditions. Renew. Energy 164, 58–73.

Atri, P.K., Modi, P., Gujar, N.S., 2020. Comparison of different MPPT control strategies for solar charge controller. In: 2020 International Conference on Power Electronics & IoT Applications in Renewable Energy and Its Control. PARC, IEEE.

Bahri, H., Harrag, A., 2021. Ingenious golden section search MPPT algorithm for PEM fuel cell power system. Neural Comput. Appl. 1–24.

Belhachat, F., Larbes, C., 2018. A review of global maximum power point tracking techniques of photovoltaic system under partial shading conditions. Renew. Sustain. Energy Rev. 92, 513–553.

Chandrasekaran, K., Sankar, S., Banumalar, K., 2020. Partial shading detection for PV arrays in a maximum power tracking system using the sine-cosine algorithm. Energy Sustain. Dev. 55, 105–121.

Fares, D., et al., 2021. A novel global MPPT technique based on squirrel search algorithm for PV module under partial shading conditions. Energy Convers. Manage. 230, 113773.

Fathabadi, H., 2020. Novel stand-alone, completely autonomous and renewable energy based charging station for charging plug-in hybrid electric vehicles (PHEVs). Appl. Energy 260, 114194.

Feroz Mirza, A., et al., 2020. Advanced variable step size incremental conductance MPPT for a standalone PV system utilizing a GA-tuned PID controller. Energies 13 (16), 4153.

Fouad, M.M., et al., 2020. Dynamic group-based cooperative optimization algorithm. IEEE Access 8, 148378-148403.

Golla, M., Chandrasekaran, K., Simon, S.P., 2021. PV integrated universal active power filter for power quality enhancement and effective power management. Energy Sustain. Dev. 61, 104–117.

Hejri, M., et al., 2014. On the parameter extraction of a five-parameter double-diode model of photovoltaic cells and modules. IEEE J. Photovolt. 4 (3), 915–923.

Humada, A.M., et al., 2016. Solar cell parameters extraction based on single and double-diode models: A review. Renew. Sustain. Energy Rev. 56, 494–509.

Ishaque, K., Salam, Z., Taheri, H., 2011a. Modeling and simulation of photovoltaic (PV) system during partial shading based on a two-diode model. Simul. Model. Pract. Theory 19 (7), 1613–1626.

Ishaque, K., Salam, Z., Taheri, H., 2011b. Simple, fast and accurate two-diode model for photovoltaic modules. Sol. Energy Mater. Sol. Cells 95 (2), 586–594.

Javed, M.Y., et al., 2019. A comprehensive review on a PV based system to harvest maximum power. Electronics 8 (12), 1480.

Kim, H., et al., 2021. A dual-mode continuously scalable-conversion-ratio SC energy harvesting interface with SC-based PFM MPPT and flying capacitor sharing scheme. IEEE J. Solid-State Circuits.

Kumar, V., et al., 2021a. A current sensor based adaptive step-size MPPT with SEPIC converter for photovoltaic systems. IET Renew. Power Gener..

Kumar, V., et al., 2021b. Load voltage-based MPPT technique for standalone PV systems using adaptive step. Int. J. Electr. Power Energy Syst. 128, 106732.

Li, Y., et al., 2020. Analysis and enhancement of PV efficiency with hybrid MSFLA–FLC MPPT method under different environmental conditions. J. Cleaner Prod. 271, 122195.

Mansoor, M., Mirza, A.F., Ling, Q., 2020a. Harris hawk optimization-based MPPT control for PV systems under partial shading conditions. J. Cleaner Prod. 122857.

Mansoor, M., et al., 2020b. Novel grass hopper optimization based MPPT of PV systems for complex partial shading conditions. Sol. Energy 198, 499–518.

Mao, M., et al., 2020. Classification and summarization of solar photovoltaic MPPT techniques: A review based on traditional and intelligent control strategies. Energy Rep. 6, 1312–1327.

Matayoshi, H., et al., 2020. Islanding operation scheme for DC microgrid utilizing pseudo droop control of photovoltaic system. Energy Sustain. Dev. 55, 95–104.

Mendez, E., et al., 2020. Improved MPPT algorithm for photovoltaic systems based on the earthquake optimization algorithm. Energies 13 (12), 3047.

Mirza, A.F., Mansoor, M., Ling, Q., 2020a. A novel MPPT technique based on henry gas solubility optimization. Energy Convers. Manage. 225, 113409.

Mirza, A.F., et al., 2019. Novel MPPT techniques for photovoltaic systems under uniform irradiance and partial shading. Sol. Energy 184, 628–648.

Mirza, A.F., et al., 2020b. A salp-swarm optimization based MPPT technique for harvesting maximum energy from PV systems under partial shading conditions. Energy Convers. Manage. 209, 112625.

Premkumar, K., et al., 2020. PSO optimized PI controlled DC-DC buck converter-based proton-exchange membrane fuel cell emulator for testing of MPPT algorithm and battery charger controller. Int. Trans. Electr. Energy Syst. e12754.

Rezk, H., Fathy, A., Abdelaziz, A.Y., 2017. A comparison of different global mppt techniques based on meta-heuristic algorithms for photovoltaic system subjected to partial shading conditions. Renew. Sustain. Energy Rev. 74, 377–386.

Shams, I., Mekhilef, S., Tey, K.S., 2020. Maximum power point tracking using modified butterfly optimization algorithm for partial shading, uniform shading, and fast varying load conditions. IEEE Trans. Power Electron. 36 (5), 5569–5581.

Srivastava, R., Tiwari, A., Giri, V., 2020. An overview on performance of PV plants commissioned at different places in the world. Energy Sustain. Dev. 54, 51–59.

Teo, J.C., et al., 2020. Impact of bypass diode forward voltage on maximum power of a photovoltaic system under partial shading conditions. Energy 191, 116491.

Tey, K.S., et al., 2018. Improved differential evolution-based MPPT algorithm using SEPIC for PV systems under partial shading conditions and load variation. IEEE Trans. Ind. Inf. 14 (10), 4322–4333.

Vicente, E.M., et al., 2020. High-efficiency MPPT method based on irradiance and temperature measurements. IET Renew. Power Gener. 14 (6), 986–995.

Yadav, K., Kumar, B., Swaroop, D., 2020. Mitigation of mismatch power losses of PV array under partial shading condition using novel odd even configuration. Energy Rep. 6, 427–437.

Yang, B., et al., 2020. Fast atom search optimization based MPPT design of centralized thermoelectric generation system under heterogeneous temperature difference. J. Cleaner Prod. 248, 119301.

Zhou, C.-g., et al., 2021. Research on MPPT control strategy of photovoltaic cells under multi-peak. Energy Rep. 7, 283–292.

Zongo, O.A., 2021. Comparing the performances of MPPT techniques for DC-DC boost converter in a PV system. Walailak J. Sci. Technol. (WJST) 18 (2), 6500(15 pages)-6500 (15 pages).